1

Planetary Masses and Orbital Parameters from Radial Velocity Measurements

C. Beaugé, S. Ferraz-Mello, and T. A. Michtchenko

Abstract

So far practically all detections of extrasolar planets have been obtained from radial velocity data, in which the presence of planetary bodies is deduced from temporal variations in the radial motion of the host star. To perform any dynamical study for these systems, it is necessary to specify: (i) initial conditions (mass and orbital elements) and (ii) an adequate coordinate system from which to construct the equations of motion. This chapter discusses both of these points.

In the first part we introduce the reader to the process of orbital determination from Doppler data, for both single and multiple exoplanetary systems. We distinguish between primary parameters (which are obtainable directly from the observational data) and secondary parameters which require additional information about the system, such as the stellar mass or inclination of the orbital plane. For multiple planetary systems we also discuss the differences between Keplerian fits, in which the mutual perturbations between the planets are neglected, and dynamical (or N-body) fits.

The second part of the chapter is devoted to the construction of the equations of motion in different coordinate systems. Special attention is given to the Hamiltonian formalism in barycentric, Jacobi and Poincaré coordinates, and we explain how to obtain orbital elements in each case. Finally, we discuss some of their advantages and disadvantages, particularly with respect to orbital fits and general dynamical studies.

1.1
Exoplanet Detection

Planets are very dim objects, and their direct observation is an extremely difficult task. Even Jupiter, the biggest planet in our own solar system, has only about 10^{-9} times the luminosity of the sun, making a similar exoplanet unobservable to us by present techniques. The first direct observation of an ex-

oplanet (*GQ Lupi*) only occurred in 2005 with VLT and, as of July 2006, three other exoplanets have also been imaged (*2M1207*, *AB Pic* and *SCR 1845*). However, most of the exoplanetary bodies have never been seen at all.

If an exoplanet cannot be seen, how can we know it is there? The basic idea is that, even if invisible, the presence of a planetary body may affect the luminosity of the star, or its motion with respect to background objects. Thus, we may deduce the existence of a planet by analyzing changes in some observable aspect of the star it revolves around. Such "indirect" detection methods are the main backbone in current discovery strategies of exoplanets. Five different techniques have been proposed and developed in recent years: (i) Stellar Transit, (ii) Radial Velocity Curves (Doppler), (iii) Gravitational Micro-lensing, (iv) Stellar Interferometry and (v) Astrometry. For details on these and other proposed methods, the reader is referred to Perryman [1] for a very comprehensive review.

Although very promising, Micro-lensing and Astrometry are still far from fulfilling their potential. Only four planetary candidates have been proposed based on micro-lensing techniques (*OGLE-05-071L*, *OGLE-05-169L*, *OGLE-05-390L* and *OGLE235-MOA53*), and even though some estimate may be obtained concerning mass and orbital period, there is no information about the remaining orbital elements. A similar picture can be given for interferometric techniques, and at present only four positive detections are counted. Astrometry has yet to yield a discovery, although the projected launch of several space telescopes (e.g., Kepler, TPF) will almost certainly change this picture. Consequently, and at least at present, practically all the currently exoplanet population has been obtained either by Stellar Transit or Doppler. The former is the subject of another chapter of this book, while the latter is the main objective of the present text.

1.2
Radial Velocity in Astrocentric Elements

The observation of a Doppler shift of the spectral lines of a star denounces a change in the velocity of the star with respect to the observer. Since the observer himself is moving with a velocity $\sim 30 \, \mathrm{km \, s^{-1}}$, variable in direction, it is necessary to subtract this motion from the observational data and reduce it to the barycenter of the solar system (for a description of the necessary operations see Ferraz-Mello et al. [2]).

The velocity of an isolated star, with respect to the barycenter of the solar system, is constant, at least for times short as compared to the timescale of galactic motion. However, if it has N planetary companions, the star will display a motion around the common barycenter of the system (see Fig. 1.1).
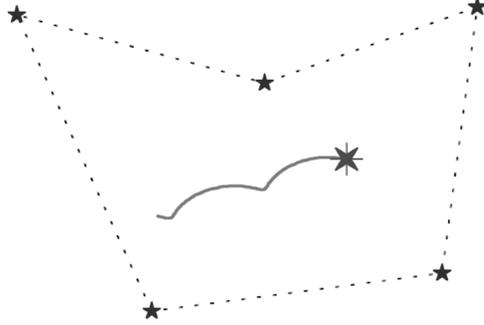
Fig. 1.1 The sinusoidal motion of a star due to the presence of a planetary companion. The faint field stars are used as a reference frame.

In order to understand this effect, we begin studying the kinematics of a single planet in elliptic orbit around the star. In an astrocentric reference frame, the position and velocity vectors of the planet are given by Brouwer and Clemence [3] and Murray and Dermott [4]:

$$\mathbf{r} = r \cos f \; \hat{\imath} + r \sin f \; \hat{\jmath} \tag{1.1}$$

$$\mathbf{v} = -\frac{2\pi a}{T\sqrt{1-e^2}} \left[\sin f \; \hat{\imath} - (e + \cos f) \; \hat{\jmath} \right]$$

where

$$r = \frac{a(1-e^2)}{1 + e \cos f} \qquad \frac{df}{dt} = \frac{2\pi a^2}{Tr^2} \sqrt{1-e^2} \tag{1.2}$$

Here r is the magnitude of the radius vector $\mathbf{r}$, the velocity vector is denoted by $\mathbf{v}$, f is the true anomaly, a is the astrocentric semi-major axis, e is the eccentricity, and $\hat{\imath}$ and $\hat{\jmath}$ are two unit vectors in the orbital plane. The first is orientated in the direction of the pericenter, and the latter is orthogonal to it. The orbital period T can be obtained directly from Kepler's third law. Denoting by m_0 the mass of the star and m the mass of the planet, we have:

$$n^2 a^3 = \mathcal{G}(m_0 + m) \tag{1.3}$$

where the mean motion $n = 2\pi/T$ is the mean angular velocity along the orbit.

We must now transform these vectors to a new coordinate system that is independent of the plane of orbital motion. For exoplanets it is customary to use a modification of the so-called Herschel astrocentric coordinates, which were first developed for studies of visual double stars. It uses the sky (i.e., a

plane tangent to the celestial sphere) as the reference plane, and a schematic view is presented in Fig. 1.2. The x-axis is taken along the intersection line between the orbital plane and the sky. Its direction is chosen towards γ, which is the node where the motion of the planet is directed towards the observer. The y-axis is also tangent to the celestial sphere, and is such that the resulting system is right-handed. Finally, the z-axis is directed along the line of sight, away from the observer.
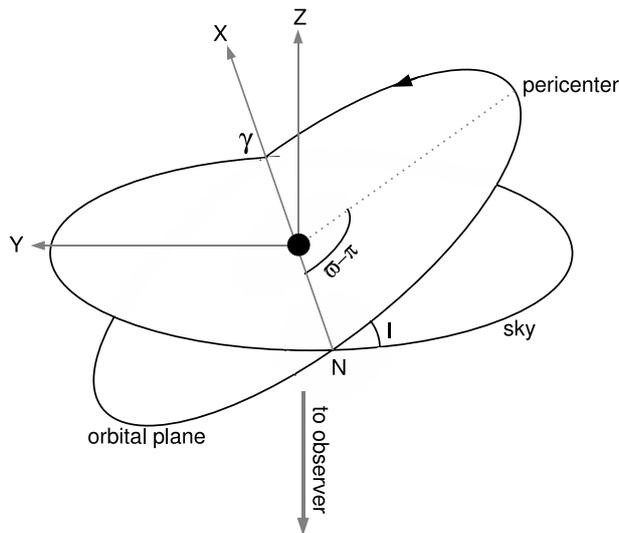
Fig. 1.2 The rotated astrocentric reference frame showing the orbital plane and the plane tangent to the celestial sphere (sky). The origin of the angles is the point γ.

In this coordinate system, the unit vectors $\hat{\imath}$, $\hat{\jmath}$ and $\hat{k}$ of the orbital plane have components:

$$\hat{\imath} = \begin{pmatrix} \cos\omega \\ \sin\omega\cos I \\ -\sin\omega\sin I \end{pmatrix} \qquad \hat{\jmath} = \begin{pmatrix} -\sin\omega \\ \cos\omega\cos I \\ -\cos\omega\sin I \end{pmatrix} \qquad \hat{k} = \begin{pmatrix} 0 \\ \sin I \\ \cos I \end{pmatrix} \qquad (1.4)$$

$\hat{k}$ is perpendicular to the orbital plane of the planet. This decomposition of the unit vectors is analogous to the transformations commonly used in celestial mechanics to pass to coordinates with respect to the ecliptic (except that here we fix $\Omega = \pi$). I is the inclination of the orbital plane with respect to the sky, and the argument of the pericenter is given by $\omega + \pi$. The addition of the angle π is due to the direction of the x-axis, which is chosen opposite to the "ascending node" N.

We can now obtain the components of **r** and **v** in this new reference frame. After a few simple algebraic manipulations, we obtain the velocity $\mathbf{v} = (v_x, v_y, v_z)$ where:

$$
\begin{aligned}
v_x &= -\frac{2\pi a}{T\sqrt{1-e^2}}\left[\sin\left(f+\omega\right)+e\sin\omega\right] \\[2mm]
v_y &= \frac{2\pi a\,\cos I}{T\sqrt{1-e^2}}\left[\cos\left(f+\omega\right)+e\cos\omega\right] \\[2mm]
v_z &= -\frac{2\pi a\,\sin I}{T\sqrt{1-e^2}}\left[\cos\left(f+\omega\right)+e\cos\omega\right]
\end{aligned}
\tag{1.5}
$$

Having the astrocentric velocity vector of the planet in the desired reference frame, we can pass to barycentric coordinates. Calling **V** the barycentric velocity vector of the planet, and $\mathbf{V}_*$ that of the star, we have that $\mathbf{v} = \mathbf{V} - \mathbf{V}_*$. On the other hand, since the barycenter is fixed in this reference frame, we have $m_0\mathbf{V}_* + m\mathbf{V} = 0$. Solving for $\mathbf{V}_*$, we obtain:

$$
\mathbf{V}_* = -\frac{m}{m_0+m}v
\tag{1.6}
$$

which represents the velocity of the motion of the star around the center of mass of the system. To calculate the velocity actually detected by the observer, we must add the velocity V_0 of the barycenter itself with respect to background stars.

It is useful to decompose this observable velocity into the tangential velocity component V_t and the radial velocity $V_r = V_{*z} + V_{0z}$. The former causes a displacement of the position of the star with respect to background stars. Its measurement is the role of astrometry but, as mentioned before, telescopes on earth are currently not able to detect these variations except in a few cases. The radial velocity V_r is far easier to detect, even with ground-based instruments, due to changes in the frequency (Doppler shift) of spectral lines from the star's spectrum. The best stellar candidates are those that, on one hand, contain a fair amount of absorption lines in the visible spectrum (i.e., must not be too hot) but, on the other hand, the number of lines must not be too large (i.e., the star must not be too cold). Thus, the best candidates are stars of spectral type F or G; in other words, similar to our own sun. A complete expression for the radial velocity can be found simply by substituting V_{*z} from Eqs. (1.5) and (1.6), and yields:

$$
V_r = \frac{2\pi a}{T\sqrt{1-e^2}}\frac{m\sin I}{(m+m_0)}\left[\cos\left(f+\omega\right)+e\cos\omega\right]+V_{r0}
\tag{1.7}
$$

where $V_{r0} = V_{0z}$ is the (constant) reference radial velocity of the barycenter.

The extension to N planets is straightforward and follows the same lines, as long as we neglect mutual perturbations and assume Keplerian solutions. We can then write the complete radial velocity of the star at a given time t as:

$$V_r(t) = \sum_{i=1}^{N} \mathcal{K}_i \left[\cos{(f_i + \omega_i)} + e_i \cos{\omega_i} \right] + V_{r0} \tag{1.8}$$

where

$$\mathcal{K}_i = \frac{m_i \sin I_i}{\mathcal{M}} \frac{2\pi a_i}{T_i \sqrt{1 - e_i^2}} \tag{1.9}$$

and

$$\mathcal{M} = \sum_{i=0}^{N} m_i \tag{1.10}$$

is the total mass of the system (star and planets). Transforming from semi-major axis to mean motions via Kepler's third law, we can then rewrite the coefficients $\mathcal{K}_i$ as:

$$\mathcal{K}_i = \left(\mathcal{G}(M + m_i) \right)^{1/3} \frac{m_i \sin I_i}{\mathcal{M}} n_i^{1/3} (1 - e_i^2)^{-1/2} \tag{1.11}$$

or, more succinctly, as

$$\mathcal{K}_i = \mathcal{F}_i(M, m_i, I_i) \qquad n_i^{1/3} (1 - e_i^2)^{-1/2} \tag{1.12}$$

where $\mathcal{F}_i(M, m_i, I_i)$ is sometimes called the "mass function" and groups all the terms that depend explicitly on the stellar and planetary masses, as well as the orbital inclination. This expression is valid only for astrocentric orbital elements. If Jacobian coordinates are employed, the expression given by Eq. (1.38) must be used.

The basis of the Doppler method is then to build an observational data base of the changes in the radial velocity of a target star. These radial velocity data points represent a discretized representation of the radial component of the left-hand side of Eq. (1.8). The idea now is to deduce, from this data set, the masses and orbital parameters of all the planetary companions that make up the right-hand member of the same equation.

Note that $V_r(t)$ is the sum of N periodic terms, each with semi-amplitude $\mathcal{K}_i$. However, the true anomaly f_i is only a linear function of time in the case of circular orbits $e_i = 0$. In the general elliptic case, only the mean anomaly ℓ_i has a constant derivative (given by the mean motion n_i). The relationship between f and ℓ is given in terms of the (intermediate) eccentric anomaly u,

and via the following two equations:

$$\tan(f/2) = \sqrt{\frac{1+e}{1-e}} \tan(u/2) \tag{1.13}$$

$$u - e\sin u = \ell = n(t - \tau)$$

The second expression is the classical Kepler equation, and must be solved iteratively to obtain the passage from ℓ (or the time) to the eccentric anomaly. The quantity τ is sometimes referred to as the time of passage through the pericenter. Finally, the mean motion n is related to the semi-major axis and masses through Kepler's third law.

As an example, Fig. 1.3 shows the shape of two fictitious radial velocity curves, constructed from Eq. (1.8) with only one planet. The continuous line shows the case of a circular orbit ($e = 0$), while the dashed line presents an example of a highly elliptic body ($e = 0.6$). Although both periods and semi-amplitudes are the same, the second curve shows distinctive peaks each time the planet crosses the pericenter of its orbital motion. Another noticeable effect of the eccentricity is a change in the averaged value of V_r. Once again, this is due to the nonlinear behavior of the true anomaly f for noncircular orbits.
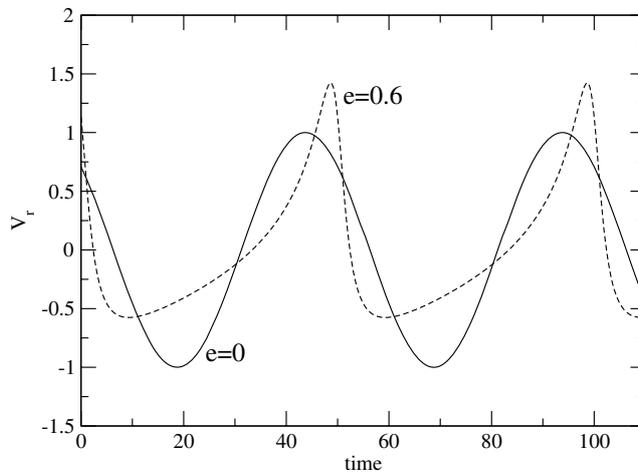
Fig. 1.3 Fictitious radial velocity curves, using Eq. (1.8) with $K = 1$, $\omega = 180$ degrees and $T = 50$ in arbitrary time units. Continuous line corresponds to a circular orbit, while the dashed curve was calculated with $e = 0.6$.

As a final important point, it must be stressed that there is no free angle equivalent to the longitude of the ascending node Ω that can be simply added to the orbital elements of the planets. As shown in Fig. 1.2, Ω measures the angular distance from the x-axis and the "ascending node" **N**, and in Herschel's

modified coordinate system it is set to $\Omega = \pi$. Expressions (1.5) for the velocity components (v_x, v_y, v_z) were derived for this orientation of the x-axis, and thus implicitly depend on this choice of Ω. Any other value for Ω would be inconsistent with the orbit issued from the observations.

1.3
## Orbital Fits from Radial Velocity Curves

1.3.1
Primary Parameters

Until recently, radial velocity data were zealously guarded by the observational teams and not available to the general scientific community. Fortunately this picture is changing (albeit slowly), and some information is currently available from the on-line versions of the published papers. This information is already pre-processed, in the sense that all the necessary steps have been taken to reduce the velocities to the barycenter of our solar system.

A real example of a radial velocity data set can be seen in Fig. 1.4 (symbols). Each point corresponds to discrete values $V_r(t_k)$ of *HD 82943*, a system known to contain two planets in a 2/1 mean-motion resonance (see Mayor et al. [5], Ferraz-Mello et al. [6]). Doppler data is usually presented in a multi-column format giving, among other information, the times of observation t_k (usually in Julian days), radial velocities $V_{rk} = V_r(t_k)$ (usually in meters per second) and the expected uncertainties ϵ_k (also in m s^{-1}). This latter values correspond to the size of the error bar of the radial velocity data, and a Gaussian error distribution is usually assumed. Current instrumentation and reduction techniques have lowered the values of ϵ_k to the order of a few m s^{-1}. When observations include data from more than one instrument, the origin of each data segment is also included in the files.

With the numerical data in hand, we first assume that the temporal variations of V_r are caused by the presence of one (or more) exoplanets, and therefore correspond to time-discrete values of a function of type (1.8). That being the case, our second task is to develop a numerical algorithm to deduce the number of periodic terms contained in the signal (i.e., number of planets N), and for each to estimate the values of the set

$$(\mathcal{K}_i, n_i, e_i, \omega_i, \tau_i) \qquad (i = 1, \ldots, N) \tag{1.14}$$

plus the barycentric radial velocity V_{r0}. These are sometimes referred to as the "primary parameters" of an orbital fit. The individual planetary masses (multiplied by $\sin I_i$) are derived from the calculated value of $\mathcal{K}_i$ and the mass function. Notice that the number of free parameters is equal to $5N + 1$, consisting of five orbital parameters per planet plus the radial velocity V_{r0} of the
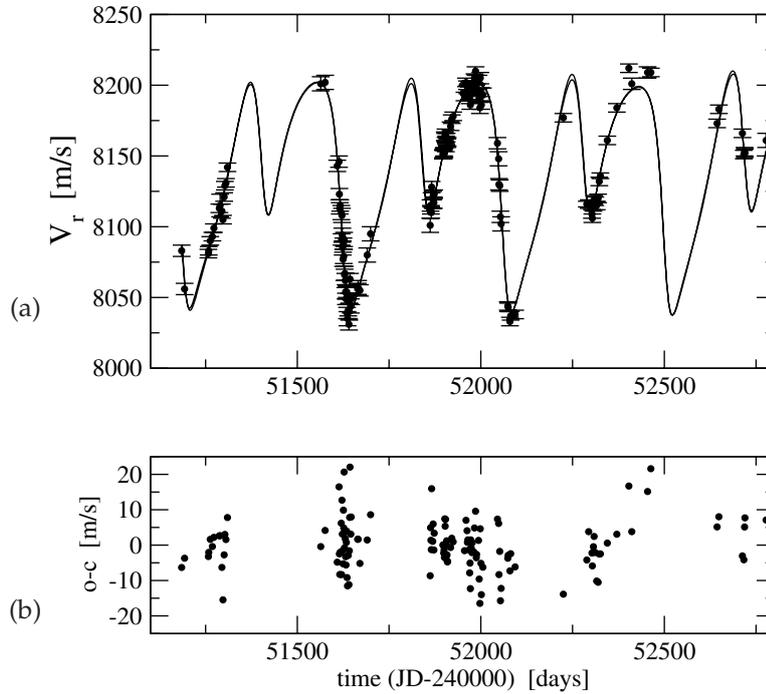
Fig. 1.4 (a) Radial velocity data points of the *HD82943* star, together with an orbital with two planets. (b) Residuals from the fit. Figure obtained with a dynamical two-planet fit.

barycenter of the extrasolar system. As we shall show later on, V_{r0} does not necessarily correspond to the time-averaged value of V_r, unless all exoplanets move in circular orbits. In the case where the data includes values from different instruments and observatories, individual values of V_{r0} are usually assigned. As a final note of caution, in the case of more than one planet, the calculated orbital periods (or mean motions) are not osculating, but apparent (see [6]).

The mass of the star is taken from sophisticated stellar models. However, one must keep in mind that, even for Hipparcos stars having the best available spectroscopy and astrometry, the more accurate models do not allow to know the masses better than $\simeq 8$ percent (Allende et al. [7]). This fact supersedes some discussions on the nature of the published planetary elements, if astrocentric or barycentric. The difference between coordinates in these systems is usually much smaller than the uncertainty in our knowledge of the stellar mass.

Even though the functional form of $V_r(t)$ given by (1.8) is the sum of periodic terms, it is not usually convenient to attempt an orbital fit using a direct

Fourier analysis. The reasons are twofold. First, a precise identification of the leading frequencies with Fourier decomposition requires that the observational data should cover several periods. This is not usually the case, specially for planets with large semi-major axis. Second, radial velocity data is not evenly spaced in the time axis and, even worse, usually contains months-long gaps where observations are not favorable. Both problems can be overcome using a more general Fourier method, such as the Dates Compensated Fourier Transform [8] or the CLEANest algorithm [9], which were specifically developed for nonequidistant data points and arbitrary frequencies. However, a least-squares algorithm is usually more precise and requires less fine-tuning of the results. Thus, practically all orbital fits have been calculated using this approach.

We then search for adequate coefficients (1.14) of a fitting function $y(t)$, of type (1.8), such that the residual function

$$Q^2 = \sum_{t_n} \frac{[y(t_n) - V_r(t_n)]^2}{\epsilon_n^2} \tag{1.15}$$

is minimum. Notice that this definition includes the uncertainty of each data point $V_r(t_n)$ and has the advantage of considering different precisions among the data. This is particularly important when mixing observations from different instruments. In the case where the ϵ_n correspond to the standard deviation of the data, Q^2 is equal to the χ^2 of the data modelization.

Initially, deterministic versions of nonlinear least-squares were used, such as hill-climbing techniques or the Levenberg–Marquardt method (see [5, 10, 11]). The main drawback with these methods is that they are unable to distinguish between local and global minima of Q^2; consequently, there is no guarantee that the calculated orbital elements correspond to the best fit of the data sets. Since the number of free parameters can be large, the shape of the residual function may be complex and contain numerous local minima, several of them possibly with similar values. Moreover, since the problem is highly nonlinear, the result may be highly sensitive to the initial values of the parameters. An example of this behavior was given by Mayor et al. [5] for the two *HD 82943* planets. The authors presented two different fits: in the first the orbital eccentricities of the planets were $(e_1, e_2) = (0.4, 0.0)$ and for the second $(e_1, e_2) = (0.4, 0.18)$. Although the eccentricity of the outer planet changed significantly, the value of Q^2 only varied by $\simeq 0.1$ percent. What is more worrisome in this case is that the best-fit solutions found by several authors actually corresponds to orbits which are dynamically unstable in timescales of the order of 10^5–10^6 years (see [6]). Thus, given a limited set of observations, the orbital configuration of the real planets does not necessarily correspond to the best fit.

Since results of orbital fits sometimes seem very sensitive to the numerical method and/or data set, we need to fine-tune our techniques. We need a strategy (or method) that can identify the global extrema of the residual function. Additionally, we must be able to estimate the confidence levels (i.e., errors) in the orbital parameters themselves. Due to the highly nonlinear characteristics of the equations, it is not correct to assume Gaussian distribution errors in $(V_{0r}, \mathcal{K}_i, n_i, e_i, \omega_i, \tau_i)$. Consequently, the standard deviations that are sometimes seen, alongside the best fits, can be misleading and must be considered with utmost care [12].

Considering that the result of classical nonlinear best-fit methods depends on the initial guess, a possible approach towards a global minimum is to apply the same method to a large number of initial conditions, distributed randomly in the parameter space. This so-called Monte Carlo approach was used by Brown [13] to the V_r data from *HD 72659*. A year later, Ferraz-Mello et al. [6] employed a similar approach to study the two-planet system of *HD 82943*. One of the main advantages of this type of Monte Carlo algorithm is the possibility of estimating the confidence region of each of the orbital elements; in other words, the different possible primary parameters that are all compatible with the given data set. For the particular case of *HD 82943*, we found a large set of different orbital fits which yield practically the same value of the residual function (see Fig. 1.5). Thus, in some cases, it is not possible to give a single value of the parameter set as the "correct" orbital fit.

A different strategy for the search of global minima of the orbital fit, is the use of genetic algorithms. This technique is based on natural selection (mimicking the behavior of biological populations), by which an initially random population of initial guesses evolves towards the global minimum. Although this approach can require larger computational resources than deterministic methods, it has proved to be extremely robust in all applications to exoplanetary systems (e.g. [14, 15]). Other advantages of this approach include its simple manipulation, and its ability to introduce non-Gaussian error estimations with no significant complications. A recommended introductory text on genetic algorithms can be found in Charbonneau [16].

1.3.2
Secondary Parameters

Whatever the chosen numerical approach, the orbital fit yields values for $V_{0r}, \mathcal{K}_i, n_i, e_i, \omega_i$ and τ_i. From these we must now estimate the planetary masses and semi-major axes. These quantities are related to the primary parameters through the Eqs. (1.3) and (1.11). Notice that we have two algebraic equations with three unknowns, and it is impossible to separate the value of $\sin I_i$ from the planetary mass. Thus, the values of m and a must be de-
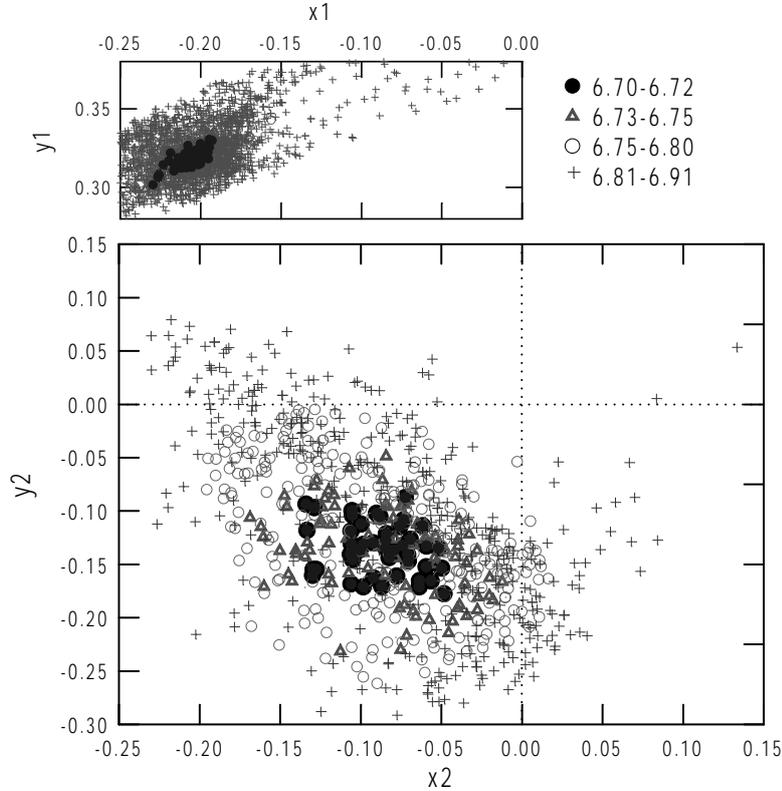
Fig. 1.5 Projections of possible orbital fits (in astrocentric orbital elements) for the two *HD 82943* planets, on the planes $(x_i, y_i) = (e_i \cos \omega_i, e_i \sin \omega_i)$. Different symbols correspond to different values of the of r.m.s. of the residuals (from Ferraz-Mello et al. [6]).

termined assuming some ad hoc value for the orbital inclination. Usually, a value of 90 degrees is chosen, which corresponds to an edge-on orbital fit and minimum planetary masses. The sensitivity of both *m* and *a* to different values of *I* is shown in Fig. 1.6. In this plot we have used the following primary parameters: $\mathcal{F} = 10^{-3}$, $M_* = 1$ and $n = 2\pi/365$ days^{-1}. Notice that both the mass and semi-major axes increase as smaller inclinations are assumed, although the mass is the most sensitive parameter. The change in *a* is not very important except for small values of *I*.

A possible determination of the real individual planetary masses occurs when both Doppler data and stellar transits are simultaneously available for an exoplanetary system. In this case, the inclination *I* is known, and *m* can be uncoupled from this angle. So far, only a handfull of exoplanets have been observed by both techniques and, for most of the rest, the masses and semi-
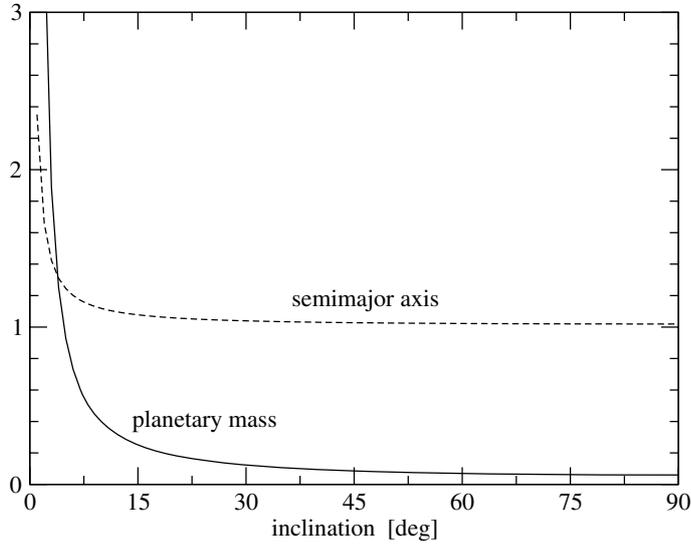
Fig. 1.6 Variation of the planetary mass m (in units of stellar mass) and semi-major axis a (in AU), as a function of the unknown inclination of the orbital plane I, for fixed values of the primary parameters of an orbital fit. The plot was constructed with $\mathcal{F} = 10^{-3}$, $M_* = 1$ and $n = 2\pi/365$ days^{-1}.

major axis are still affected by I_i. At first hand, this seems a major limitation for any dynamical analysis, since these are probably the most important parameters. However, if for multiple planetary systems we assume that all planets are co-planar, then the ratios:

$$\frac{m_j}{m_i} \qquad \frac{a_j}{a_i} \qquad\qquad (i, j = 1, \ldots, N) \qquad\qquad (1.16)$$

are unaffected by the value of the spatial inclination. In other words, although the individual values of m_i and a_i may be unknown, the relative values can be deduced, and used in our dynamical studies.

1.3.3
N-Body Fits

In the previous analysis, we have assumed that the motion of each planet orbiting a given star can be modeled by a Keplerian ellipse. This is an approximation since mutual perturbations will cause the orbital elements to change with time. If the estimated values for the planetary masses (minimum values) are sufficiently small or the mutual separation (i.e., a_i/a_j) are sufficiently large, we can assume that the orbital variations are negligible within the timespan of the observations. In that case, the multi-Keplerian fits presented before are

valid approximations to the problem. However, if the mutual perturbations are large, we must modify the orbital fit to accommodate nonconstant orbital elements. This is usually referred to dynamical (or N-Body) orbital fits.

We assume a data file consisting of several observations, starting at time $t = t_0$ and ending at $t = t_M$. In this interval, the orbital elements are allowed to vary with time. A dynamical fit proceeds the same way as the multi-Keplerian version, except for the calculation of the model values of $V_r(t_i)$. For perturbed orbits, it is no longer optimal to use (1.8) to relate the radial velocity with the orbital elements. The procedure can be separated into the following steps:

1. Specify initial conditions $(n_{i0}, e_{i0}, \omega_{i0}, \tau_{i0}, I_{i0})$ for all the planets, which will correspond to the astrocentric orbits at the beginning of the observations. The orbital period of each planet must be osculating, and not apparent [6]. We will also require values for the real planetary masses, unaffected by the inclinations I_i.

2. Transform the orbital elements to Cartesian coordinates and velocities. We will need Kepler's third law to obtain the semi-major axes, and thus the result will depend on the stellar mass m_0. From this data we can calculate the velocity vector of the star **V** (with respect to the barycenter of the system) at t_0. Choosing the reference frame of the coordinate system tangent to the celestial sphere, the first model value of $V_r(t_0)$ will be given by the z-component of **V**.

3. Using an N-body numerical integrator, calculate the positions of the planets at all the subsequent times of observation (i.e., $t = t_1, \ldots, t_M$).

4. For each t_i, repeat the calculations in Step 2, and obtain the complete set of radial velocities $V_r(t_i)$.

Having all the values of $V_r(t_i)$ for the chosen initial conditions and real planetary masses, we can calculate the residual function. The best fit will then be the set of initial parameters $(n_{i0}, e_{i0}, \omega_{i0}, \tau_{i0}, I_{i0})$ and planetary masses that minimizes Q^2. The use of numerical integrations will obviously increase the amount of CPU time; thus N-body fits are sometimes done as a second-order approximation from initial Keplerian parameters.

A factor to be taken into account is the uncertainty in the value of the stellar mass, and its propagation to other quantities in the orbital fit. To obtain a_i we must use Kepler's third law, and the results depend explicitly on the choice of m_0. A possible way to avoid these problems is to use an adimensional formulation for the equations of motion (see [2]). Even if this approach is not employed, it can easily be seen that the ratios m_i/m_j and a_i/a_j between any two planets are unaffected by the particular value of m_0. The same characteristic was also seen in the dependence of the orbital fits with the inclinations I.

Thus, any dynamical study that can be constructed as a function of these ratios will yield results virtually independent of I and m_0.

One of the most important traits of dynamical fits is its theoretical ability to assess the planetary masses independently of other detection methods, thus allowing us to bypass the limitations of radial velocity data. However, this task is not always possible. Even for fixed edge-on systems, the difference between a dynamical and a multi-Keplerian fit is appreciable only if: (i) the planets are under significant mutual perturbations and, (ii) the observational timespan is large. This is true only in a very few cases, the most well known example being *GJ 876* [10]. For almost all other known planetary systems, the distinction is practically unnoticeable.

An example is given in Fig. 1.7 for the *HD 82943* planets. We can see little difference between both fits (Keplerian and dynamical) within the observation interval and, at least for this system, both models yield similar results. However, the divergence between results will increase with time, and longer observational timespans should be able to detect the effects of mutual perturbations between the planets.
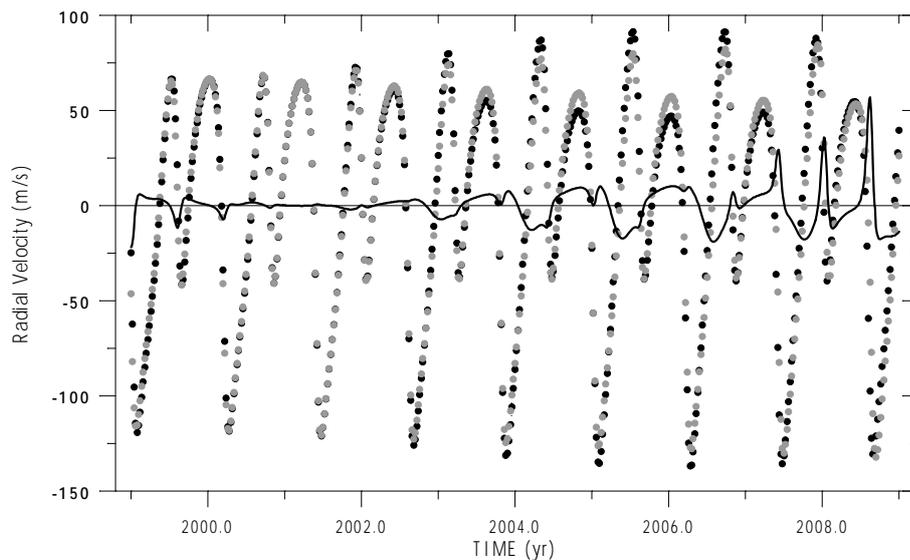
Fig. 1.7 Reconstruction of the radial velocity curve for *HD 82943*, from a multi-Keplerian fit (gray dots) and an N-body fit (black dots). The solid line shows the difference (Keplerian minus dynamical). For more details, see Ferraz-Mello et al. [6].

Since dynamical fits are not necessary for most planetary systems, in practice we are still not able to decouple the planetary masses from the inclinations. The values of I_i are not usually considered variables, but fixed at some

initial value, and co-planarity between the planets is assumed. Thus, the true potential of N-body fits is still far from being fulfilled. Once again, however, larger observational timespans will certainly change this picture.

1.4
Coordinate Systems and Equations of Motion

Even with all the limitations and uncertainties, stemming both from the observations and reduction techniques, orbital fits yield (minimum) masses and orbital elements of the planets in a given stellar system. As a first step towards a dynamical study, we must construct their equations of motion.

Suppose a system consisted of a star of mass m_0 and N planets of mass m_i, thus making this a $(N + 1)$-body problem. Let X_i denote the position vectors of all bodies with respect to an inertial reference frame centered in the barycenter of the system. Then, from Newton's law of gravitation, we have:

$$\ddot{X}_i = -\mathcal{G} \sum_{\substack{j = 0 \\ j \neq i}}^{M} m_j \frac{X_i - X_j}{|X_i - X_j|^3} \tag{1.17}$$

where the double dot denotes the second derivative with respect to the time. Introducing the astrocentric positions of the planets as $r_i = X_i - X_0$, we can write the equations of motion for the planets in astrocentric variables as:

$$\ddot{r}_i = -\mathcal{G} \frac{(m_0 + m_i)}{|r_i|^3} r_i + \mathcal{G} \sum_{\substack{j = 1 \\ j \neq i}}^{M} m_j \left(\frac{r_j - r_i}{|r_j - r_i|^3} - \frac{r_j}{|r_j|^3} \right) \tag{1.18}$$

In terms of these coordinates, the barycentric motion of the star is given by:

$$X_0 = -\frac{\sum_{i_1}^{N} m_i r_i}{\sum_{i_1}^{N} m_i} \tag{1.19}$$

The second term inside the brackets is due to the noninertiality of the astrocentric reference frame, and is caused by the perturbations of the planets on the motion of the star.

1.4.1
Barycentric Hamiltonian Equations

Since dynamical studies of extrasolar planets benefit from the Hamiltonian structure of the equations of motion, we devote the rest of this section to

presenting three different forms of canonical variables and Hamiltonian functions. Although this is a well established problem in celestial mechanics, the vast majority of papers deal with the so-called restricted problem in which only two bodies have finite masses.

The barycentric Hamiltonian equations of the $(N + 1)$-body problem are easy to obtain from Eq. (1.17). Defining $\mathbf{\Pi}_i = m_i \dot{\mathbf{X}}_i$ as the linear momenta associated to each position vector $\mathbf{X}_i$, these variables are canonical, and the Hamiltonian of the system is the sum of their kinetic and potential energies:

$$\tilde{H} = \frac{1}{2} \sum_{k=0}^{N} \frac{\Pi_k^2}{m_k} - \mathcal{G} \sum_{k=0}^{N} \sum_{j=k+1}^{N} \frac{m_k m_j}{\Delta_{kj}} \tag{1.20}$$

where $\Delta_{kj} = |\mathbf{X}_k - \mathbf{X}_j|$. This system has, however, $3(N + 1)$ degrees of freedom, that is, six equations more than the usual Laplace–Lagrange formulation of the heliocentric equations of motion.

The system can be reduced to $3N$ degrees of freedom through the convenient use of the trivial conservation laws concerning the inertial motion of the barycenter. There are two sets of variables used to reduce to $3N$ the number of degrees of freedom of the above system. Each will be discussed in the following subsections.

1.4.2
Jacobi Hamiltonian Formalism

The most popular reduction, due to Jacobi, is widely used in the study of the general three-body problem and of planetary and stellar systems. In Jacobi's formulation, the position and velocity of the planet m_1 are given in a reference frame with origin in m_0 (equal to the star); the position and velocity of m_2 are given in a reference frame with the origin at the barycenter of m_0 and m_1; the position and velocity of m_3 are given in a reference frame with the origin at the barycenter of m_0, m_1 and m_2, and so on. If we denote with $\boldsymbol{\rho}_k \ (k = 1, \ldots, N)$ the vectors thus defined, we have

$$\boldsymbol{\rho}_k = \mathbf{X}_k - \frac{1}{\sigma_k} \sum_{j=0}^{k} m_j \mathbf{X}_j \qquad (k = 1, \ldots, N) \tag{1.21}$$

where

$$\sigma_k = \sum_{j=0}^{k} m_j \tag{1.22}$$

The quantities $\boldsymbol{\rho}_k$ are our new coordinates; we must now search for their canonical momenta $\boldsymbol{\pi}_k$. These can be obtained from the original $\boldsymbol{p}_k$ by means

of the simple canonical condition $\sum_{i=1}^{N}(\boldsymbol{\pi}_i d\boldsymbol{\rho}_i - \boldsymbol{\Pi}_i dX_i) = 0$, and give the implicit relation:

$$\boldsymbol{\Pi}_k = \pi_k - \sum_{j=k+1}^{N} \frac{m_k \pi_j}{\sigma_{j-1}} \qquad (1.23)$$

The reader is referred to Ferraz-Mello et al. [2] for details of this construction. A lengthy, but simple calculation shows that nonconstant terms of the total kinetic energy, in these variables, are given by

$$T = \sum_{i=1}^{N} \frac{\pi_i^2}{2\tilde{\beta}_i} \qquad (1.24)$$

where $\tilde{\beta}_i$ are the so-called reduced masses of the Jacobian formulation, defined by

$$\tilde{\beta}_i = \frac{m_i \sigma_{i-1}}{\sigma_i} \qquad (1.25)$$

The complete Hamiltonian of the relative motion of the N planets, can be written as:

$$H = H_0 + H_1 \qquad (1.26)$$

where:

$$H_0 = \sum_{k=1}^{N} \left(\frac{\pi_k^2}{2\tilde{\beta}_k} - \frac{\mathcal{G}\sigma_k \tilde{\beta}_k}{\rho_k} \right) \qquad (1.27)$$

$$H_1 = -\mathcal{G} \sum_{k=1}^{N} \sum_{j=k+1}^{N} \frac{m_k m_j}{\Delta_{kj}} - \mathcal{G} \sum_{k=1}^{N} m_k \left(\frac{m_0}{\Delta_{0k}} - \frac{\sigma_{k-1}}{\rho_k} \right)$$

Constant terms were discarded, since they do not contribute to the equations. This function defines a system with $3N$ degrees of freedom in the canonical variables (ρ_k, π_k) with $(k = 1, \ldots, N)$.

Notice that H_0 may be written as the sum of N terms of the form

$$F_k = \frac{\pi_k^2}{\tilde{\beta}_i} - \frac{\mathcal{G}\sigma_k \tilde{\beta}_k}{\rho_k} \qquad (1.28)$$

each of which represents the Hamiltonian for the unperturbed motion of m_k around the center of gravity of the first $(k-1)$ mass-points. It is easy to see that it has the same functional form as the two-body Hamiltonian in astrocentric coordinates, except for a change of definition in the masses. Thus, the solution of the unperturbed system with $H_1 = 0$ are also conics, and we can

use (1.28) to define new *Jacobian* orbital elements. These will differ from their astrocentric counterparts in the first order of the planetary masses.

1.4.3
Poincaré Hamiltonian Formalism

A different reduction to $3N$ degrees of freedom is due to Poincaré [17]. The resulting equations were not often used in studies of the solar system, perhaps because Poincaré himself mentioned he believed its difficulties outweighted its advantages [18]. However, in recent years this approach has been applied successfully to several problems in planetary dynamics [19–22]. In fact, and as we will show below, Poincaré's formalism is not so complex at all and, when compared to Jacobi's approach, the expressions are significantly simpler, and even easier to use.

The definition of the new canonical variables (r_i, p_i) for the N planets are very simple. The new coordinates r_i are simply equal to the astrocentric position vectors $X_i - X_0$, and the new momenta p_i are the same linear momenta Π_i of the barycentric formulation. Hence,

$$r_i = X_i - X_0 \qquad p_i = \Pi_i \qquad (i = 1, 2, \ldots, N) \tag{1.29}$$

It is noteworthy that this definition mixes coordinate systems, the positions being astrocentric while the momenta are barycentric.

We refer the reader to [2] for more details on the construction of these variables, as well as the algebraic manipulations to obtain the Hamiltonian function. The works of Laskar [19] and Laskar and Robutel [20] are also highly recommended references.

The Hamiltonian of the reduced system can once again be written as $H = H_0 + H_1$, where

$$H_0 = \sum_{i=k}^{N} \left(\frac{1}{2} \frac{p_k^2}{\beta_k} - \frac{\mu_k \beta_k}{r_k} \right) \tag{1.30}$$

$$H_1 = \sum_{k=1}^{N} \sum_{j=k+1}^{N} \left(-\frac{\mathcal{G} m_k m_j}{\Delta_{kj}} + \frac{p_k \cdot p_j}{m_0} \right)$$

and

$$\mu_k = \mathcal{G}(m_0 + m_k) \qquad \beta_k = \frac{m_0 m_k}{m_0 + m_k} \tag{1.31}$$

We note that H_0 is of the order of the planetary masses m_k while H_1 is of order two with respect to these masses. Then H_0 may be seen as the new expression for the undisturbed energy while H_1 is the potential energy of the interaction

between the planets. It is worth noting that each term

$$F_k = \frac{1}{2}\frac{p_k^2}{\beta_k} - \frac{\mu_k \beta_k}{r_k} \tag{1.32}$$

is the Hamiltonian of a two-body problem in which the mass point m_k is moving around the mass point m_0.

The expression for the perturbation term H_1 is worth a couple of comments. On one hand, it is more compact than its counterpart in Jacobi coordinates (Eq. (1.27)). In fact, it is very similar to the expression of the disturbing function in the astrocentric reference frame. If we add a greater simplicity of the definition of the canonical variables, Poincaré's approach begins to appear more appealing than Jacobi's. On the other hand, Poincaré's expression for H_1 includes terms that depend on the momenta, and this characteristic is baffling to a first-time user. Most of us are used to working with potentials that are only a function of the positions, and mixed variables have the feel of non-conservative systems. The explanation, however, simply lies in the different reference frames chosen for the coordinates and momenta.

1.4.4
Generalized Orbital Elements and Delaunay Variables

The reduced Hamiltonians (1.27) and (1.30) were written in Cartesian coordinates. The purpose of this subsection is to obtain "general" orbital elements and Delaunay variables corresponding to both Jacobi and Poincaré formalisms.

Orbital elements (or their Delaunay canonical counterparts) of each planetary mass m_i are defined as solutions of each F_i making up the unperturbed Hamiltonian H_0. The expression for F_i in each coordinate system is:

$$\text{Astrocentric} \quad : \quad F_k = \frac{1}{2}\frac{(m_k \dot{r}_k)^2}{m_k} - \frac{\mathcal{G}(m_0 + m_k)m_k}{r_k}$$

$$\text{Jacobi} \quad : \quad F_k = \frac{1}{2}\frac{\pi_k^2}{\tilde{\beta}_k} - \frac{\mathcal{G}\sigma_k \tilde{\beta}_k}{\rho_k} \tag{1.33}$$

$$\text{Poincar} \quad : \quad F_k = \frac{1}{2}\frac{p_k^2}{\beta_k} - \frac{\mu_k \beta_k}{r_k}$$

Recall, however, that astrocentric coordinates $(r_k, m_k \dot{r}_k)$ are only canonical if $N = 2$, while the Jacobi and Poincaré version are canonical for any number of bodies.

Notice that all three expressions in (1.33) have the same functional form with respect to the coordinates; only the mass parameters are different. This means that the solution in each coordinate system will also have the same

form, and their integrals of motion (e.g., orbital elements) can be obtained with the same formulas. In particular, we can write a general expression for F_k in the form:

$$F_k = \frac{1}{2}mv^2 - \frac{\mu}{|\boldsymbol{r}|} \tag{1.34}$$

where the meaning of the set $(\boldsymbol{r}, \boldsymbol{v}, m, \mu)$ in each reference frame is summarized in Table 1.1.

Table 1.1 Correspondence between coordinates and mass parameters defining the unperturbed Hamiltonian H_0 in three different reference frames.

Coordinate system	Position ($\boldsymbol{x}$)	Velocity ($\boldsymbol{v}$)	Mass (m)	μ
Astrocentric	$\boldsymbol{r}_k$	$\dot{\boldsymbol{r}}_k$	m_k	$\mathcal{G}(m_0 + m_k)$
Jacobi	$\boldsymbol{\rho}_k$	$\boldsymbol{\pi}_k/\tilde{\beta}_k$	$\tilde{\beta}_k$	$\mathcal{G}\sigma_k$
Poincaré	$\boldsymbol{r}_k$	$\boldsymbol{p}_k/\beta_k$	β_k	μ_k

We can now use the usual two-body formulas to define generalized orbital elements in each reference frame. These expressions can be found in any textbook on celestial mechanics (e.g., [3, 4, 23]). For the semi-major axis and eccentricity, we have:

$$a \stackrel{\text{def}}{=} \frac{\mu r}{2\mu - rv^2}$$

$$e \stackrel{\text{def}}{=} \sqrt{\left(1 - \frac{r}{a}\right)^2 + \frac{(\boldsymbol{r} \cdot \boldsymbol{v})^2}{\mu a}} \tag{1.35}$$

The remaining elements also follow the same usual definitions. Kepler's Third Law also reads:

$$n^2 a^3 = \mu \tag{1.36}$$

where, once again, the different definitions of μ yield different relations between the semi-major axis and orbital frequency. Last of all, we need to modify the orbital elements $(a, e, I, l, \omega, \Omega)$ to a canonical set. The usual choice is the so-called mass-weighted Delaunay variables $(L, G, T, l, \omega, \Omega)$, where the new momenta are defined by:

$$L = m\sqrt{\mu a}$$

$$G = L\sqrt{1 - e^2} \tag{1.37}$$

$$T = G\cos I$$

It is interesting to note that Eqs. (1.35) and (1.36) are valid for all our reference systems; the only difference lies in the definitions found in Table 1.1 for each individual case.

1.4.5
Comparisons Between Coordinate Systems

We have seen that, at least formally, the Poincaré formalism is simpler and more compact than the Jacobi variables. But how does each perform in practice? We have simulated the short-term orbital evolution of a co-planar system formed by a central star with $m_0 = 0.32 M_\oplus$ and two planets with masses $m_1 = 20 M_{\text{Jup}}$ and $m_2 = 5 M_{\text{Jup}}$. Initial conditions were chosen such that both planets have circular orbits with semi-major axes $a_1 = 0.131$ AU and $a_2 = 0.232$ AU and are in opposition. The large planetary masses were chosen in order to have strong perturbations and to avoid misleading graphics hiding the actual behavior of the orbital parameters.

Figure 1.8 shows the variations of the semi-major axis (a) and eccentricity (b) of the outer planet only. The orbital elements were calculated in each of the three reference frames (astrocentric, Jacobi and Poincaré). The inner planet shows very little difference, and is not shown. The results noted in Fig. 1.8 should be taken with care. The Jacobi variables are those showing the less variable elements in this example, but this is due to the fact that the planet in the innermost orbit is much larger. Thus, the results appearing here can differ from system to system and depend on the arbitrary order in which the planets are chosen in the construction of Jacobian coordinates. When a natural choice is possible, as in the given example, Jacobi elements are those showing the least variations.

The main advantage of having a small temporal variation, at least on short timescales, can be found in orbital fits. If the two-body values of a and e vary little, then a multi-Keplerian orbital determination from radial velocity data will be more precise than a case where the same parameters show significant variations throughout the observational interval. For these reasons, in recent years Jacobi coordinates have been a popular choice for orbital determination. The only problem lies in the hierarchical structure of Jacobi coordinates. In order to define the variables, we must first know which is the first planet, which is the second, etc. This prior knowledge is not necessary in Poincaré or astrocentric variables, and can lead to confusion or erroneous results if not done with care.

Orbital fits in Jacobi coordinates can be undertaken in the same way as deduced for astrocentric elements, except for a change in the definition of the semi-amplitudes K_i. Thus, the complete radial velocity of the star m_0 is still

given by (1.8), but now:

$$\mathcal{K}_i = \frac{m_i \sin I_i}{\sigma_i} \frac{2\pi a_i}{\hat{T}_i \sqrt{1 - e_i^2}} \qquad \text{with} \qquad \hat{T}_i = \frac{2\pi a_i^{3/2}}{\sqrt{\mathcal{G} \sigma_i}} \tag{1.38}$$

and where $\sigma_i = \sum_{k=0}^{i} m_i$, and all orbital elements are Jacobian. The reader is referred to Lee and Peale [24] for further details.

In conclusion, Jacobi seems a good choice for orbital representation, especially if N-body fits are not employed. However, the larger sensitivity of the astrocentric coordinates to mutual perturbations has its advantages. If dynamical fits are used in the hope of uncoupling the planetary masses and the inclinations, astrocentric coordinates are preferable, since the orbital varia-
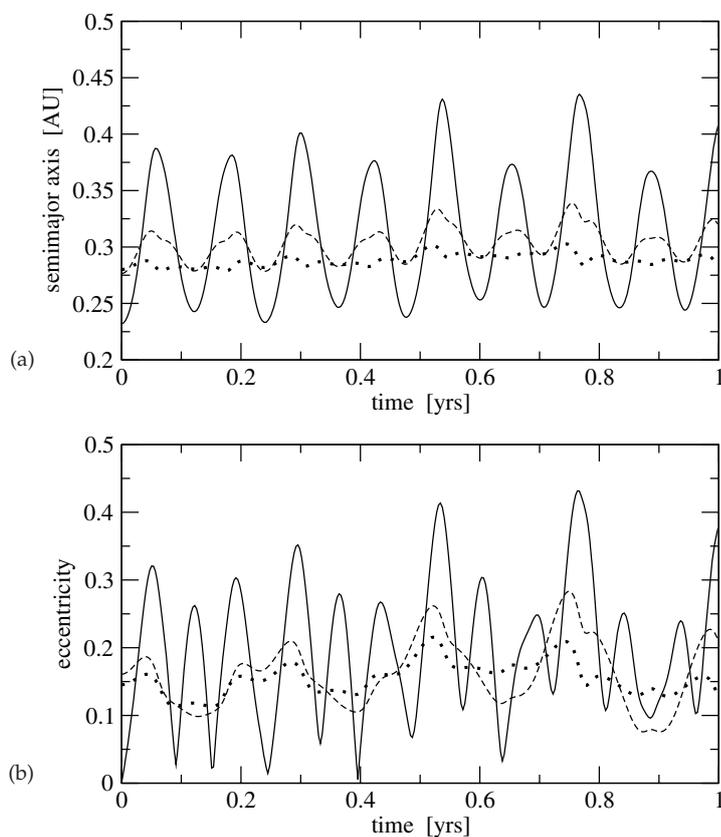
Fig. 1.8 Evolution of semi-major axis and eccentricity of the outer body (two-planet system) in three different coordinate systems. Continuous lines correspond to astrocentric orbital elements, dotted lines to Jacobi variables, and dashed lines to orbital elements deduced from Poincaré canonical variables.

tions will first become appreciable in this reference frame. Thus, the choice between Jacobi and astrocentric for the process of orbital determination depends on the problem at hand, and on the information desired by the researcher. Whatever the choice, the Poincaré canonical variables still stands out as the most adequate reference frame for dynamical studies. The transformation between all systems is straightforward, and there should not be any inhibitions in using different coordinates for different tasks.

1.4.6
The Conservation of the Angular Momentum

If the only forces acting on the $N + 1$ bodies are their point-mass gravitational attractions, the angular momentum is conserved:

$$\mathcal{L} = \sum_{i=0}^{N} m_i \mathbf{X}_i \times \dot{\mathbf{X}}_i \tag{1.39}$$

Since $\sum i = 0^N m_i \mathbf{X}_i = \sum i = 0^N m_i \dot{\mathbf{X}}_i = 0$, the above equation gives

$$\mathcal{L} = \sum_{i=0}^{N} m_i \mathbf{r}_i \times \mathbf{p}_i \tag{1.40}$$

which, in terms of the orbital elements, yields

$$\mathcal{L} = \sum_{i=1}^{N} \beta_i \sqrt{\mu_i a_i (1 - e_i^2)} \mathbf{k}_i \tag{1.41}$$

where $\mathbf{k}_i$ are the unit vectors normal to the orbital planes. This is an exact conservation law. In this equation a_i and e_i are not the usual astrocentric osculating elements but the canonical Poincaré elements.

The conservation law given by (1.40) is also true if Jacobian coordinates are used. It is worth emphasizing that when a_i and e_i are the astrocentric osculating elements, the expression

$$\hat{\mathcal{L}} = \sum_{i=1}^{N} m_i \sqrt{\mu_i a_i (1 - e_i^2)} \mathbf{k}_i \tag{1.42}$$

is no longer an exact conservation law. One may easily see that:

$$\hat{\mathcal{L}} = \mathcal{L} - \sum_{i=1}^{N} m_i \mathbf{X}_0 \times \dot{\mathbf{X}}_0 \tag{1.43}$$

showing that the quantity $\hat{\mathcal{L}}$ has in fact a variation of order $\mathcal{O}(m_i^2)$. Thus, the conservation of the total angular momentum can only be obtained in canonical variables, and not in astrocentric orbital elements.

References

1 Perryman, M.A.C.: 2000, Extra-solar planets. *Rep. Prog. Phys.*, **63**, 1209–1272.

2 Ferraz-Mello, S., Michtchenko, T.A., Beaugé, C. and Callegari Jr., N.: 2005b, Extrasolar Planetary Systems. In *Chaos and Stability in Planetary Systems*, (R. Dvorak, F. Forester and J. Kiths, Eds.), Lect. Notes Phys., **683**, 219–271.

3 Brouwer, D. and Clemence, G.M.: 1961, *Methods of Celestial Mechanics*, Academic Press, NY.

4 Murray, C.D. and Dermott, S.F.: 1999, *Solar System Dynamics*, Cambridge University Press.

5 Mayor, M., Udry, S. Naef, D., Pepe, F., Queloz, D., Santos, N.C. and Burnet, M.: 2004, The CORALIE survey for southern extrasolar planets. XII. Orbital solutions for 16 extrasolar planets discovered with CORALIE. *A&A*, **415**, 391–402.

6 Ferraz-Mello, S., Michtchenko, T.A. and Beaugé, C.: 2005a, The orbits of the extrasolar planets HD 82943c and b. *ApJ*, **621**, 473.

7 Allende Prieto, C. and Lambert, D.L.: 1999, Fundamental parameters of nearby stars from the comparison with evolutionary calculations: masses, radii and effective temperatures. *A&A*, **352**, 555–562.

8 Ferraz-Mello, S.: 1981, Estimation of periods from unequally spaced observations. *AJ*, **86**, 619–624.

9 Foster, G.: 1995, The cleanest Fourier spectrum. *AJ*, **109**, 1889–1902.

10 Laughlin, G. and Chambers, J.E.:2001, Short-term dynamical interactions among extrasolar planets. *ApJ*, **551**, L109–L113.

11 Rivera, E. and Haghighipour, N.: 2006, On the stability of test particles in extrasolar multiple planetary systems. *MNRAS*, in press.

12 Ford, E.B.: 2005, Quantifying the uncertainty in the orbits of extrasolar planets. *AJ*, **129**, 1706–1717.

13 Brown, R.A.: 2004, New information from radial velocity data sets. *ApJ*, **610**, 1079–1092.

14 Stepiński, T.F., Malhotra, R. and Black, D.C.: 2000, The upsilon Andromeda system: models and stability. *ApJ*, **545**, 1044–1057.

15 Goździewski, K. and Migaszewski, C.: 2006, About putative Neptune-like extrasolar planetary candidates. *A&A*, **449**, 1219–1232.

16 Charbonneau, P.: 1995, Genetic algorithms in astronomy and astrophysics. *ApJSS*, **101**, 309–334.

17 Poincaré, H.: 1897, Sur une forme nouvelle des équations du problème des trois corps. *Bull. Astron.*, **14**, 53.

18 Poincaré, H.: 1905, *Leçcons de Mécanique Céleste*, Gauthuer-Villars, Paris, Vol. I.

19 Laskar, J.: 1991, In *Predictability, Stability and Chaos in N-Body Dynamical Systems*, Plenum Press, NY, pp. 93.

20 Laskar, J. and Robutel, P.: 1995, Stability of the planetary three-body problem. I. Expansion of the planetary Hamiltonian. *CMDA*, **62**, 193–217.

21 Michtchenko, T.A. and Ferraz-Mello, S.: 2001, Modeling the 5:2 mean-motion resonance in the Jupiter–Saturn planetary system. *Icarus*, **149**, 357–374.

22 Beaugé, C. and Michtchenko, T.A.: 2003, Modelling the high-eccentricity three-body problem. Application to the GJ876 planetary system. *MNRAS*, **341**, 760–770.

23 Ferraz-Mello, S.: 2007, *Canonical Perturbation Theories, Degenerate Systems and Resonance*, Springer.

24 Lee, M.H. and Peale, S.J.: 2003, Secular evolution of hierarchical planetary systems. *ApJ*, **592**, 1201–1216.